J Mater Sci (2007) 42:2662–2668
DOI 10.1007/s10853-006-1361-4

Microstructural study of carbonized wood after cell wall sectioning

Kengo Ishimaru · Toshimitsu Hata · Paul Bronsveld · Yuji Imamura

Received: 21 September 2005 / Accepted: 27 February 2006 / Published online: 4 January 2007

Abstract Wooden blocks of Japanese cedar (*Cryptomeria japonica)* were carbonized at 700 and 1,800 °C. The microstructure was analyzed by transmission electron microscopy (TEM) and μ-Raman spectroscopy of the inner planes of wood cell walls. The predominant structure was of a turbostratic nature and no heterogeneity was observed originating from the original cell walls. TEM observations of samples carbonized at 1,800 °C showed ordered regions in the surface layer of cell walls. This result was supported by polarized μ-Raman analysis. It may be caused by the deposition of carbon compounds volatilized from the cell walls during pulse current heating.

Introduction

Wood is composed mainly of the polysaccharides cellulose, hemicellulose, and lignin and behaves therefore as an aromatic compound [1]. A unique characteristic stems from the layered structure of microfibrillar cellulose and its components distributed heterogeneously in cell walls [1]. In recent years, the microstructure of wood before and after carbonization is considered to be an important topic for the control of wood-based carbon materials [2, 3] and as biomorphous template for the formation of SiC and SiC/C composites [4–6]. However, there are so far only a few studies focused on the microstructure in the cell walls of carbonized wood [4, 7–9].

In a recent study of wood carbonization, Byrne and Nagle predicted a preferred orientation of the carbon crystallites from the shrinkage of wood cell walls during carbonization [7]. Paris also reported a weak preferred orientation of the carbon crystallites parallel to the cell axis during carbonization [8]. On the other hand, Otani discussed the connection of the main wood components with the multi-phase graphitization of carbonized wood from an X-ray diffraction study and concluded that it is not caused by the constitutional heterogeneity of wood [10]. In this study, we try to clarify the relationship between the characteristic structure of a wood cell wall and the microstructure of carbonized wood. Therefore, the microstructure in a cell wall for wood carbonized at 700 and at 1,800 °C was investigated in detail by scanning electron microscopy (SEM), transmission electron microscopy (TEM) and by polarized μ-Raman spectroscopy.

Experimental

Wooden blocks of Japanese cedar (*Cryptomeria japonica*) with the size of approximately $12 \times 12 \times 20$ mm^3 dried at 105 °C for 24 h were heated to 700 °C with a heating rate of 4 °C/min in a laboratory scale electric furnace. The samples were kept constant for 1 h at the

K. Ishimaru (✉)
Central Research Laboratory, Daiwa House Industry Co., Ltd, 631-0801, Nara, Japan
e-mail: k-ishimaru@daiwahouse.jp

K. Ishimaru · T. Hata · Y. Imamura
Research Institute for Sustainable Humanosphere (RISH), Kyoto University, Gokasho, 611-0011, Uji, Japan

P. Bronsveld
Department of Applied Physics, University of Groningen, Groningen, The Netherlands

temperature in a N_2 gas flow and then cooled to room temperature. Sample shrinkage took place to the amount of 23% in axial direction, 30% in radial direction and 33% in tangential direction. After putting the sample preheating at 700 °C in a graphite mold, it was heated from room temperature to 1,800 °C with a heating rate of 15 °C/min and kept constant for 30 min at the temperature in a current-heating device (Plasman, S S Alloy, Hiroshima) under vacuum [6]. Electric current was applied directly to the sample through a graphite die.

The morphology of the samples before and after carbonization was studied in a SEM (JEOL JSM-5310) operating at 10 kV. The samples were observed directly without any coating.

TEM samples embedded in epoxy resin were cut parallel to the cell axis at the tangential section of the cell walls at a thickness of about 40 nm by an ultramicrotome and a diamond knife, shown in Fig. 1a. TEM observations were made with a 100 kV transmission electron microscope (JEOL JEM-200EXII).

Raman spectra of the carbonized samples were recorded at room temperature with a Renishaw inVia Raman spectroscope equipped with an air-cooled CCD detector. An argon laser (λ = 514.5 nm) was adopted as an excitation source. The laser was focused to approximately 1 μm in diameter at a power of less than 1 mW at the sample surface in order to prevent irreversible thermal degradation. Typical measuring points on the cell walls are shown in Fig. 1b. There are tangential and longitudinal planes imaged as indicated in Fig. 1b. Spot A, B, and C corresponds to the center position, the corner position, and the inner surface of cell walls as shown in Fig. 1b, respectively. Also polarized Raman spectra were recorded with the Raman spectroscope using a

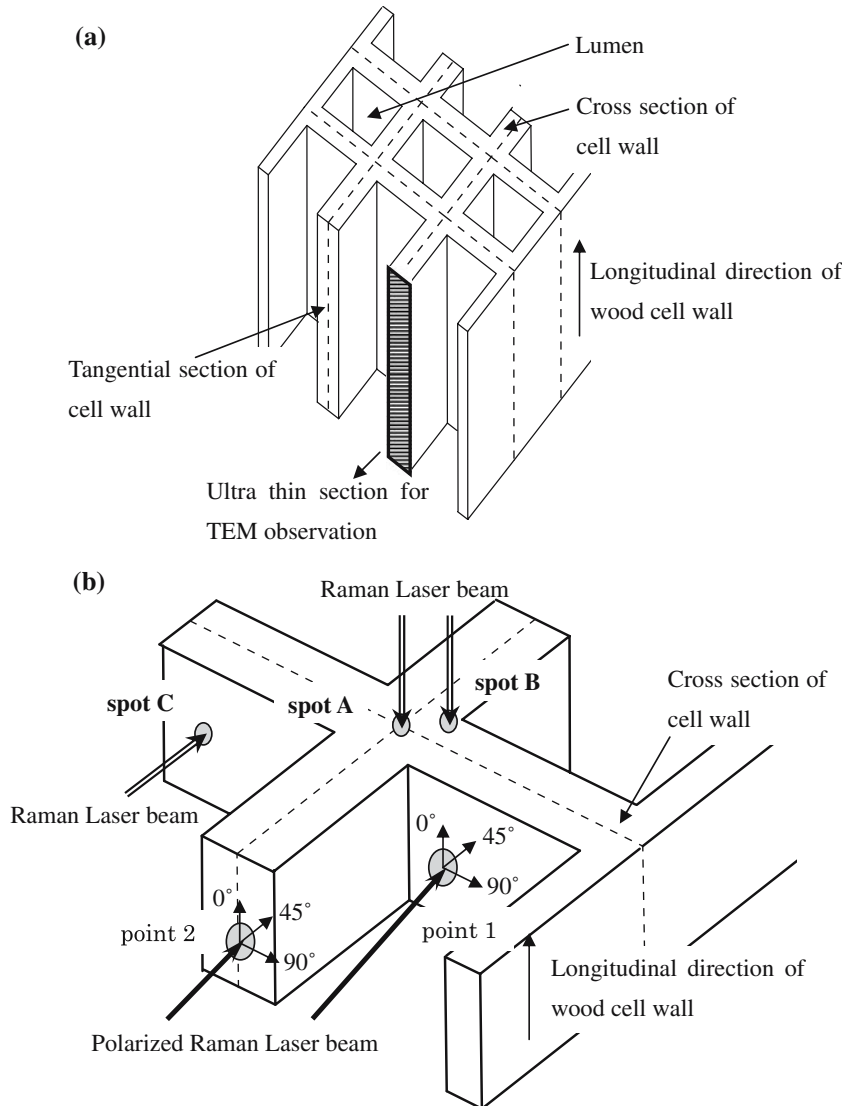

Fig. 1 Schematic diagram of TEM sample preparation (**a**) and (un)polarized Raman analysis (**b**)

532 nm YAG laser, focused to a spot of 2–3 μm using a 50× magnifying lens. To collect the polarized Raman spectra, the incident laser beam was passed through a polarizer and focused onto the sample. The laser in the Raman spectrometer was polarized and fixed parallel to the axial direction of the wood cell wall. The rotation angle of a sample was changed manually from 0° to 45° to 90°, where 0° corresponded to the axial direction of the wood cell wall, as shown in Fig. 1b.

The polarized and unpolarized Raman spectra were recorded more than three times for each analysis point in order to check sample damage by laser irradiation and at three different points on a sample under the same measuring condition to avoid spurious changes in spectral intensities. All polarized and unpolarized Raman spectra were measured in the 1,000–1,800 cm^{-1} zone and fitted using a mixed Gaussian/Lorentzian function. The wave number was calibrated using the 520 cm^{-1} line of a silicon wafer.

Results and discussion

Figure 2 shows SEM images of the cross section of cell walls for wood before (a) and after carbonization at 700 °C (b). In non-carbonized Japanese cedar, a discrete cell wall consists of a secondary wall and a compound middle lamella, see Fig. 2a. The secondary wall in raw wood cell wall structure consists of quite a high density of microfibrillar cellulose while the highest density of lignin components is located in the compound middle lamella of raw wood cell walls [1]. In the carbonized sample, cell walls still do exist, but without any visible lamella substructure, see Fig. 2b. Figure 3a, b shows bright field TEM images for an ultra thin tangential plane of cell walls in wood carbonized at 700 and 1,800 °C, respectively. Indeed, no cell wall substructure could be observed.

Figures 4 and 5 show 002 dark field (DF) images in an ultra thin tangential plane of cell walls carbonized at 700 and 1,800 °C, respectively. At 700 °C, 002 DF images as depicted in Fig. 4b shows a large amount of bright domains of approximately 1–2 nm in size attributed to small carbon crystallites of hexagonal carbon layers [11–13]. Carbon crystallites were homogeneously distributed and little difference was observed in the size of carbon crystallites in the cell wall. Carbon crystallites were homogeneously distributed and little variation was observed in the size of them. At 1,800 °C, 002 DF images as depicted in Fig. 5b represent carbon crystallites about 3–8 nm in size [11]. Still no heterogeneous distribution or size differences of carbon crystallites could be observed.

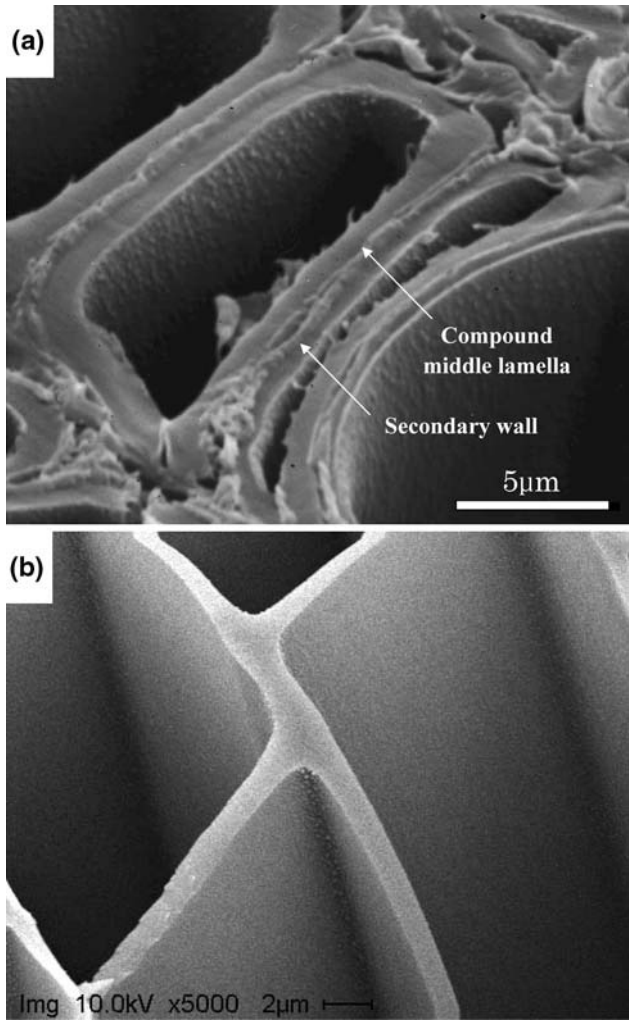

Fig. 2 SEM images of cell wall for wood before (**a**) and after carbonization at 700 °C (**b**)

Figure 6 shows Raman spectra on these same inner surfaces. The two common Raman bands corresponding to the in-plane vibrations of sp^2-bonded carbon with structural imperfections (D band) and those of the crystalline vibrations of sp^2-bonded carbon (G band) were distinctively observed at the positions of approximately 1,350 cm^{-1} and 1,580–1,600 cm^{-1}, respectively [14, 15].

The position of the Raman G band, the full width at half maximum (FWHM) of the Raman G and D bands, and the peak intensity ratio of G and D (I_d/I_g) are the characteristic Raman parameters for the carbon structure of carbonaceous materials [8, 14, 15]. Table 1 shows the values of these Raman parameters at spot A, B and C for samples carbonized at 700 and 1,800 °C. The position of the Raman G band is shifted to 1,580 cm^{-1}, the FWHM of the Raman G and D bands are decreased from 700 °C to 1,800 °C, and the I_d/I_g

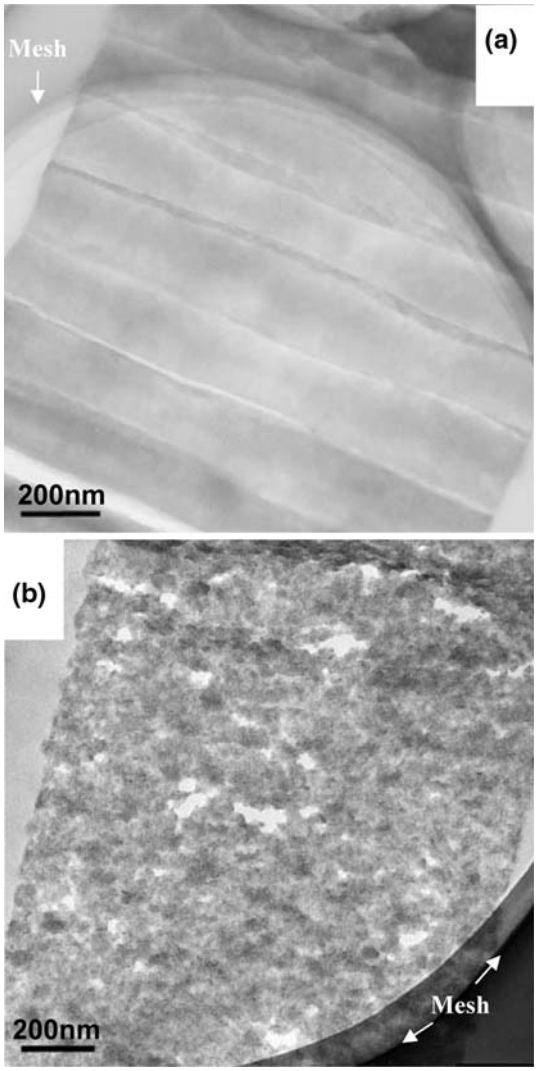

Fig. 3 Bright field (BF) TEM images for an ultra thin tangential plane of cell walls for wood carbonized at 700 °C (**a**) and 1,800 °C (**b**). Dark curved shape in the upper part in (**a**) and in the lower right in (**b**) is a part of lacy carbon mesh

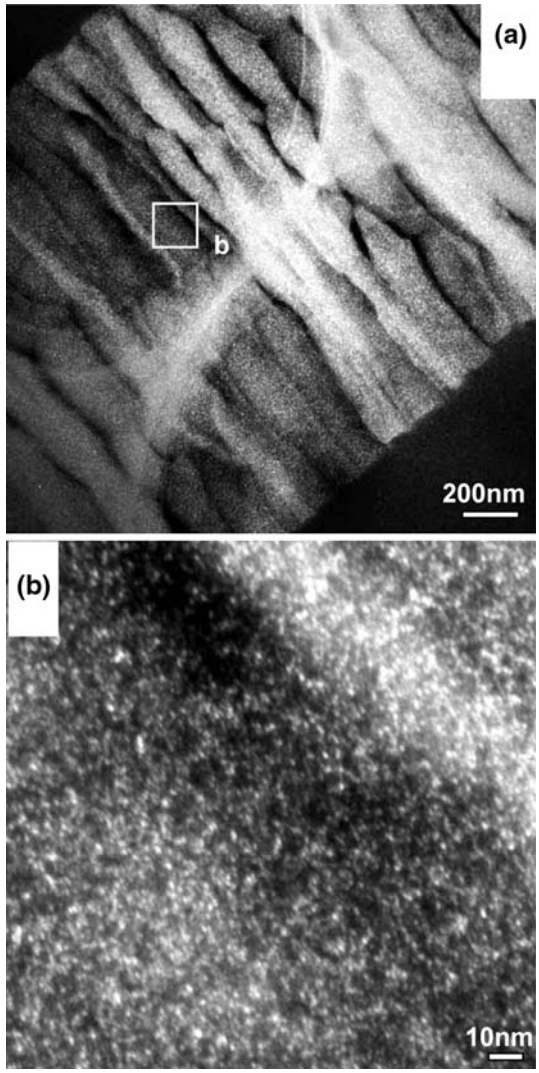

Fig. 4 (002) Dark field (DF) TEM images for an ultra thin tangential plane of cell walls in wood carbonized at 700 °C: (**a**) Low magnification image of overall view of cell wall, (**b**) selected image in the square of b in (**a**). Bright curved shape in the center of (**a**) is a part of lacy carbon mesh

ratio increased. At first site, three points have to be addressed in Table 1. A poorly developed D-band at 700 °C giving rise to a large D-FWHM and a low I_d/I_g, a rather big increase in this ratio going from 700 °C to 1,800 °C, and finally a substantial difference between the value for the intensity ratio for spots A and B on the one hand versus the value for spot C. First of all at 700 °C, the D-band is hardly developed so that the FWHM is high and the I_d/I_g small. Moreover, Raman data similar to Fig. 6b taken between 700 °C and 1,800 °C very clearly indicate that the Raman D-band becomes stronger than the G-band with higher heat treatment temperature, due to the strongly increase in the number of defects. For an improvement in the degree of order in the carbon crystallites we expect the G-band to increase and its FWHM to decrease [14, 15]. In disordered carbon materials, the I_d/I_g is inversely proportional to the development of the carbon crystallites during carbonization [8, 16]. The conclusion must be that defect production and carbon crystallite growth are competing with each other.

There was little difference in carbon structure between cell wall center (spot A) and cell wall edge (spot B) for both temperatures, as shown in Table 1. Thus, the constitutional heterogeneity in the wood cell wall hardly affects the distribution and size of carbon crystallites in the cell wall. That does not hold for the inner surface of cell walls (spot C in Table 1) for the sample carbonized at 1,800 °C. All Raman parameters on the inner surface of cell walls (spot C) showed a

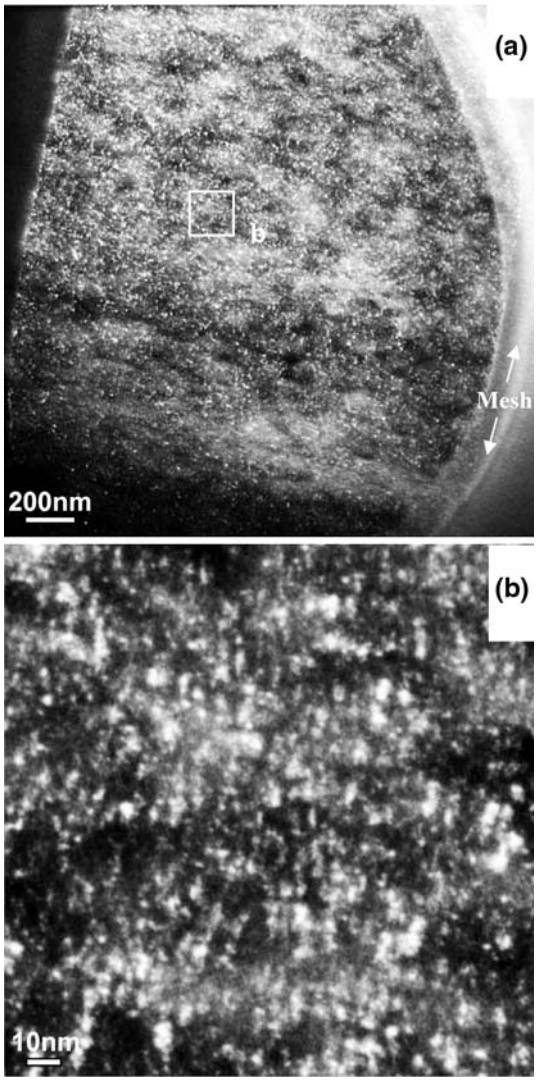

Fig. 5 (002) DF TEM images for an ultra thin tangential plane of cell walls in wood carbonized at 1,800 °C: (**a**) Low magnification image of overall view of cell wall, (**b**) selected image in the square of b in (**a**). Bright curved shape in the right end of (**a**) is a part of lacy carbon mesh

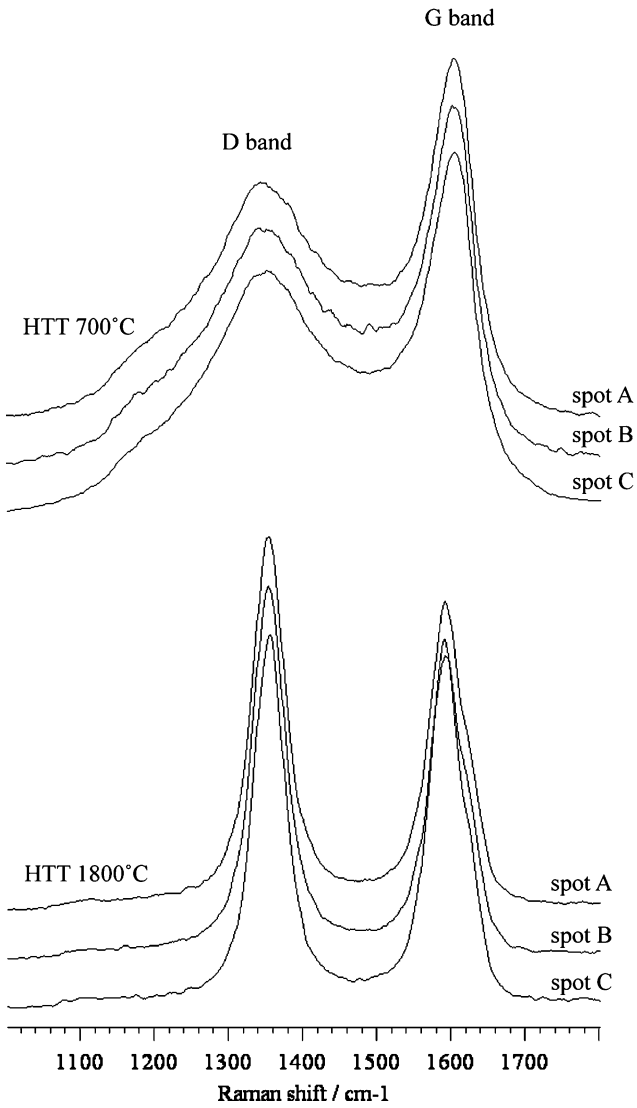

Fig. 6 Raman spectra at the position of the inner surface and cross section of cell walls (spots A, B, and C in Fig. 1b) of the samples carbonized at 700 and 1,800 °C

slightly better ordering in the orientation of carbon crystallites compared with those on the cross section of cell walls (spot A and B). Thus, spot-like polarized Raman analysis confirmed the presence of ordering in orientation of carbon crystallites on the inner surface of a cell wall of the sample carbonized at 1,800 °C

Preferred orientation of carbon crystallites in an ultra thin tangential plane of cell walls of the sample carbonized at 1,800 °C was also demonstrated in the TEM images of Fig. 7a, b when the objective aperture position was rotated from parallel (0°) to perpendicular (90°) to the longitudinal direction of a cell wall [11]. At 0° of the objective aperture, only carbon crystallites fulfill the 002 Bragg conditions which lie parallel to the cell surface. These TEM images show a slightly preferred orientation of carbon crystallites parallel to the inner surface of a cell wall, as shown in Fig. 7a. Carbon crystallites perpendicular to the longitudinal direction of cell walls were hardly observable at the inner surface of cell walls, as depicted in Fig. 7b. Thus, a slight preference for the orientation parallel to the cell wall surface and in the longitudinal direction of a cell wall was observed in the sample at 1,800 °C.

In addition, Fig. 8 shows a BF TEM image for an ultra thin tangential plane of cell walls with clear evidence for a preferred orientation in the top layer. Thus, these TEM results indicate the existence of ordering of carbon crystallites in the inner surface of a

Table 1 Raman parameters at the position of spot A, B, and C in Fig. 1b of cell wall on carbonized wood at 700 and 1,800 °C

HTT (°C)	Beam spot position	G position (cm^{-1})	G FWHM (cm^{-1})	D FWHM (cm^{-1})	*Id*/*Ig*
700	Spot A	1,602	60	181	0.52
	Spot B	1,602	60	181	0.52
	Spot C	1,602	61	181	0.53
1,800	Spot A	1,591	47	52	1.34
	Spot B	1,592	48	53	1.35
	Spot C	1,587	44	51	1.03

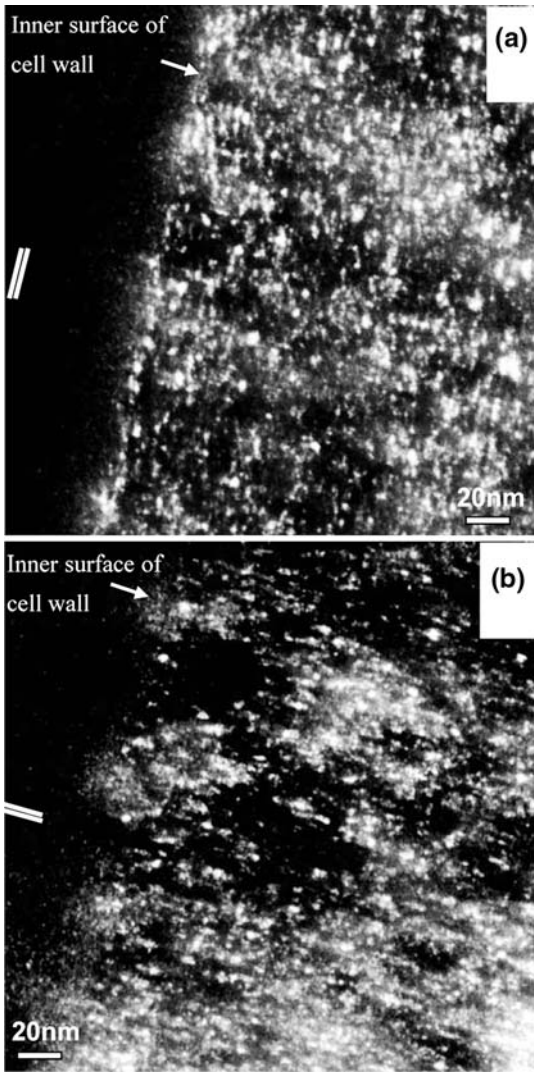

Fig. 7 Orthogonal (002) DF TEM images in an ultra thin tangential plane of cell walls carbonized at 1,800 °C. 0° and 90° (**a**, **b**) of aperture position along the cell axis. The orientation of aromatic layers in carbon crystallites is represented by a double bar

cell wall along the longitudinal direction for samples carbonized at 1,800 °C.

This difference in ordering of carbon crystallites between in the inner surface and the tangential section

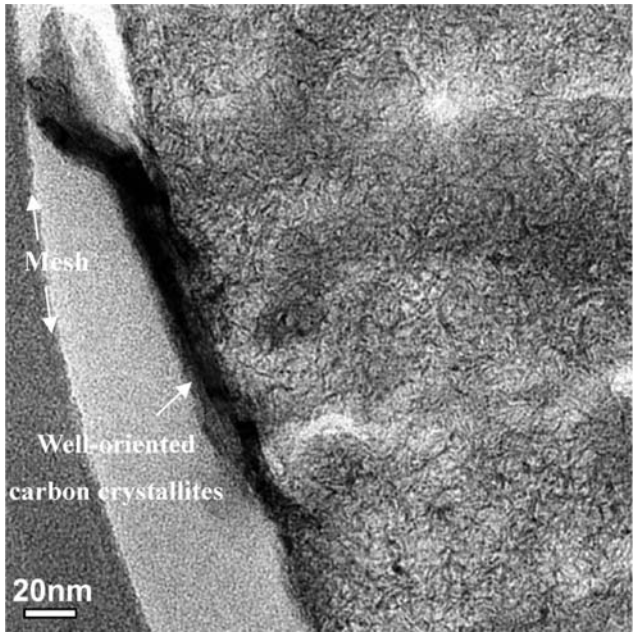

Fig. 8 BF TEM image at the inner surface of cell walls in an ultra thin tangential plane of cell walls carbonized at 1,800 °C. Circular black contract at the lower left in Fig. 7 is lacy carbon mesh

of cell walls of the sample carbonized at 1,800 °C was also investigated by polarized micro-Raman spectroscopy. Figure 9 shows typical polarized Raman spectra at different sample angles on the inner surface of a cell wall (Point 1 in Fig. 1b). In Table 2, a comparison is made between the Raman parameters obtained from polarized Raman spectra at different sample angles for point 1 and 2 of the sample carbonized at 1,800 °C.

What strikes the eye is the fact that for all Raman parameters there is almost no dependence on the angular position but that the I_d/I_g values for point 1 are significantly lower than for point 2. The orientation of carbon crystallites both on the inner surface and the tangential section of a cell wall seem to be basically random. However, polarized Raman parameters on the inner surface of a cell wall (point 1) showed a preferred ordering in orientation of carbon crystallites compared with those on the tangential section (point 2), which is

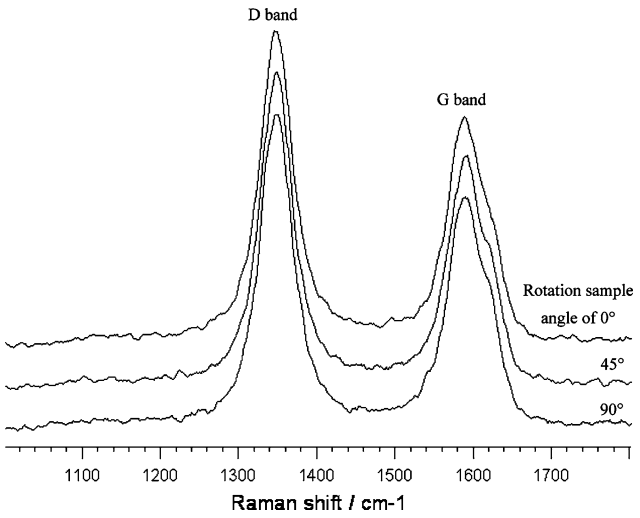

Fig. 9 Polarized Raman spectra on the inner surface of cell wall of the sample carbonized at 1,800 °C at the different sample angles

Table 2 Raman parameters obtained from polarized Raman spectra of wood carbonized at 1,800 °C

Analysis point	Rotation angle	G position (cm^{-1})	G FWHM (cm^{-1})	D FWHM (cm^{-1})	*Id*/*Ig*
Point 1	0°	1,87	48	50	1.44
	45°	1,588	52	52	1.42
	90°	1,587	49	49	1.44
Point 2	0°	1,589	55	52	1.63
	45°	1,589	53	50	1.61
	90°	1,590	55	50	1.62

in good agreement with the results of Raman analysis and TEM observation, shown in Table 1, Figs. 7 and 8.

The formation mechanism may be explained as follows: gasses released from the sample during heat treatment by pulse current heating are redeposited along the surface of the cell wall inside the lumen. The weight loss of the sample after carbonization up to 1,800 °C by pulse current heating was 4.9%. This result may indicate the presence of volatile products with low molecular weight compounds during heat treatment up to 1,800 °C. Pyrolysis gasses released from cell walls are condensing onto cell lumen walls giving rise to well-oriented carbon depositions.

Paris et al. [8] reported that the developing carbon crystallites show a weak preferred orientation with respect to the cell axes of the carbonized wood up to 1,400 °C. Otani and Oya [10] reported that multi-phase graphitization occurs in carbonized wood above 2,600 °C, but not necessarily caused by the constitutional heterogeneity of wood. This study suggests that the well-ordered orientation of carbon crystallites along a cell wall of wood carbonized at 1,800 °C is related to the preferred orientation of them along a cell wall and multi-phase graphitization of the carbonized wood.

Conclusions

The microstructure in cell walls of wood carbonized at 700 and 1,800 °C was studied by SEM, TEM and polarized μ-Raman spectroscopy. The discrete cell wall layers of raw wood were no longer observed at 700 °C. SEM- and TEM-observations confirmed that the microstructure of a cell wall for carbonized wood was turbostratic in nature without any heterogeneity originating from the constitutional heterogeneity of wood. However, well-ordered carbon crystallites were observed on the inner surface of a cell wall for a sample carbonized at 1,800 °C. This surface layer could be formed by deposition of vaporized carbon gasses on the surface of cell walls during heat treatment and may play an important role in the formation of preferred orientation of carbon crystallites and multi-phase graphitization of carbonized wood at high temperatures.

Acknowledgements The authors are grateful to Dr. Junji Sugiyama, RISH, for the experimental support with TEM. We are also thankful to Shuichi Muraishi, Renishaw and Toyoko Imai, Zeon Corporation, for the experimental support with polarized micro Raman Analysis. This research was carried out with support from Grant-in-Aid for Scientific Research (14002121) from the Ministry of Education, Science, and Culture of Japan.

References

1. Lewin M, Goldstein I (1991) In: Wood structure and composition. Marcel Dekker, Inc., New York, p 149
2. Hata T, Vystavel T, Bronsveld P, DeHosson J, Kikuchi H, Nishimiya K, Imamura Y (2004) Carbon 42:961
3. Hata T, Ishimaru K, Fujisawa M, Bronsveld P, Vystavel T, Hosson JD, Kikuchi H, Nishizawa T, Imamura Y (2005) Nanotubes Carbon Nanostruct 13:435
4. Greil P, Lifka T, Kaindl A (1998) J Eur Cera Soc 18:1961
5. Fujisawa M, Hata T, Bronsveld P, Castro V, Tanaka F, Kikuchi H, Furuno T, Imamura Y (2004) J Eur Ceram Soc 24:3575
6. Castro V, Fujisawa M, Hata T, Bronsveld P, Vystavel T, Hosson JD, Kikuchi H, Imamura Y (2004) Key Eng Mat 264–268:2267
7. Byrne CE, Nagle DC (1997) Carbon 35:267
8. Paris O, Zollfrank C, Zickler GA (2005) Carbon 43:53
9. Kercher AK, Nagle DC (2003) Carbon 41:15
10. Otani S, Oya A (1971) Tanso 64:10 [in Japanese]
11. Shiraishi M, Terriere G, Oberlin A (1978) J Mat Sci 13:702
12. Oberlin A (1979) Carbon 17:7
13. Huttepain H, Oberlin A (1990) Carbon 28:103
14. Katagiri G, Ishida H, Ishitani A (1988) Carbon 26:565
15. Cuesta A, Dhamelincourt P, Laureyns J, Martinez-Alonso A, Tascon JMD (1994) Carbon 32:1523
16. Yamauchi S, Kurimoto Y (2003) J Wood Sci 49:235